processes

MDPI

Article

Depositional Environment Changes during the Cenozoic in the Northeastern Margin of the Qinghai–Tibet Plateau

Yetong Wang [1,2,*], Guoqiang Sun [2,3,*], Shuncun Zhang [2,3], Irene Cantarero [4], David Cruset [5], Vinyet Baqués [4], Hui Guo [2,3], Shangshang Bo [1,2] and Anna Travé [4]

1 University of Chinese Academy of Sciences, Beijing 100049, China; boshangshang21@mails.ucas.ac.cn
2 Northwest Institute of Eco-Environment and Resources, Chinese Academy of Sciences, Lanzhou 730000, China; zhangshuncun@lzb.ac.cn (S.Z.); guohui@nieer.ac.cn (H.G.)
3 Key Laboratory of Petroleum Resources, Lanzhou 730000, China
4 Departament de Mineralogia, Petrologia i Geologia Aplicada, Facultat de Ciències de la Terra, Universitat de Barcelona (UB), C/Martí i Franquès s/n, 08028 Barcelona, Spain; i_cantarero@ub.edu (I.C.); vbaques@ub.edu (V.B.); atrave@ub.edu (A.T.)
5 Group of Dynamics of the Lithosphere, Geo3BCN–CSIC, Lluís Solé i Sabaris s/n, 08028 Barcelona, Spain; dcruset@geo3bcn.csic.es
* Correspondence: wangyetong16@mails.ucas.edu.cn (Y.W.); sguoqiang@lzb.ac.cn (G.S.)

Abstract: The uplift of the Tibetan Plateau (TP) during the late Cenozoic is thought to be one of the crucial factors controlling the Asian climate. However, the complex interaction between tectonics and climate change remains unclear. The carbon and oxygen isotopes and elementary geochemistry of rocks from the early Eocene Lulehe Formation to the Miocene Youshashan Formation in the northern margin of Qaidam Basin, shows important variations in the Rb/Sr, MgO/CaO, Sr/Cu, and V/Cr ratios, together with CMI and CIA, which are interpreted as reflecting relevant regional climate and environmental changes. Combining the above mentioned parameters, we reconstructed the evolution of the sedimentary environment in the Qaidam Basin. The climate is roughly divided into four stages: (1) warm and humid; (2) cold and dry; (3) alternations of cold and dry with warm and humid; and (4) cold and arid. At the same time, there are also minor short-term changes of dry, wet, cold, and warm in each stage. The early Eocene to Miocene climate changes in the Qaidam Basin were mainly affected by global climate changes, the uplift of the Qinghai Tibet Plateau, and the long-lasting plate collision, but there was no continuous drought due to the uplift of the Qinghai Tibet Plateau. From the early Eocene to the late Miocene, the climate of the Qaidam Basin became warm and humid.

Keywords: Cenozoic climate; trace elements; isotope analysis; Qaidam Basin; Qinghai–Tibet Plateau

Citation: Wang, Y.; Sun, G.; Zhang, S.; Cantarero, I.; Cruset, D.; Baqués, V.; Guo, H.; Bo, S.; Travé, A. Depositional Environment Changes during the Cenozoic in the Northeastern Margin of the Qinghai–Tibet Plateau. *Processes* **2022**, *10*, 1000. https://doi.org/10.3390/pr10051000

Academic Editors: Alon Kuperman and Alessandro Lampasi

Received: 6 April 2022
Accepted: 14 May 2022
Published: 18 May 2022

1. Introduction

The subduction and collision of the Indian plate changed the tectonic framework of the Eurasian plate, forming the Qinghai–Tibet Plateau and a series of sedimentary basins around it [1]. At the same time, the uplift of the Tibetan Plateau also triggered climate change in Asia, and even the world [2]. The Qinghai–Tibet Plateau is located at the junction of the eastern monsoon region, the western arid region, and the plateau cold region, which makes it extremely sensitive to climate changes, and its sediments are important carriers for recording past climate changes [3,4]. The huge amount of Cenozoic sediments deposited in the basins around the Qinghai–Tibet Plateau are natural materials for studying uplifting, tectonic evolution, and climate changes.

The geochemical characteristics of sedimentary rocks are good tracers of environmental changes [5]. With the development of analysis and testing technology, the method of applying element geochemistry to analyze the paleoenvironment and paleotemperature is becoming more and more mature [6–10]. Previous researchers have used the color of sediments, paleontology, and carbon and oxygen isotopes to study the sedimentary environment of different Cenozoic successions in the northeastern margin of the Tibetan

Plateau [11–14], but there is no sufficient continuous geochemical evidence for the Cenozoic stratigraphic system in the Qaidam Basin. The low degree of detailed characterization and lack of long-scale sedimentary environment evolution limit the large-scale comparative study between different basins in western China.

In this paper, the Cenozoic sedimentary environment of the Qaidam Basin was studied by means of the environment-sensitive geochemical indicators and the sedimentary environment evolution model of the northwest margin of Qaidam Basin is established. This paper also provides case examples of strategies that can be employed to evaluate the ratios of Rb/Sr, MgO/CaO, Sr/Cu, V/Cr, CMI, and CIA in studies of climate changes and sedimentary environments.

2. Geological Setting

The Qaidam Basin, located in the northeastern margin of the Qinghai–Tibet Plateau, is the largest Cenozoic inland basin in this Plateau (Figure 1) [15]. The Qaidam Basin and its surrounding tectonic units are separated by large fault zones. To the northwest, the Altun strike-slip fault separates this Plateau from the Tarim Basin, the Kunlun Central fault zone separates the Plateau from the East Kunlun orogenic belt in the south, the Zongwulong fault zone separates the Plateau from the Qilian Mountains in the northeast, and the Wenquan fault separates the Plateau from the Gonghe Basin in the east [16].

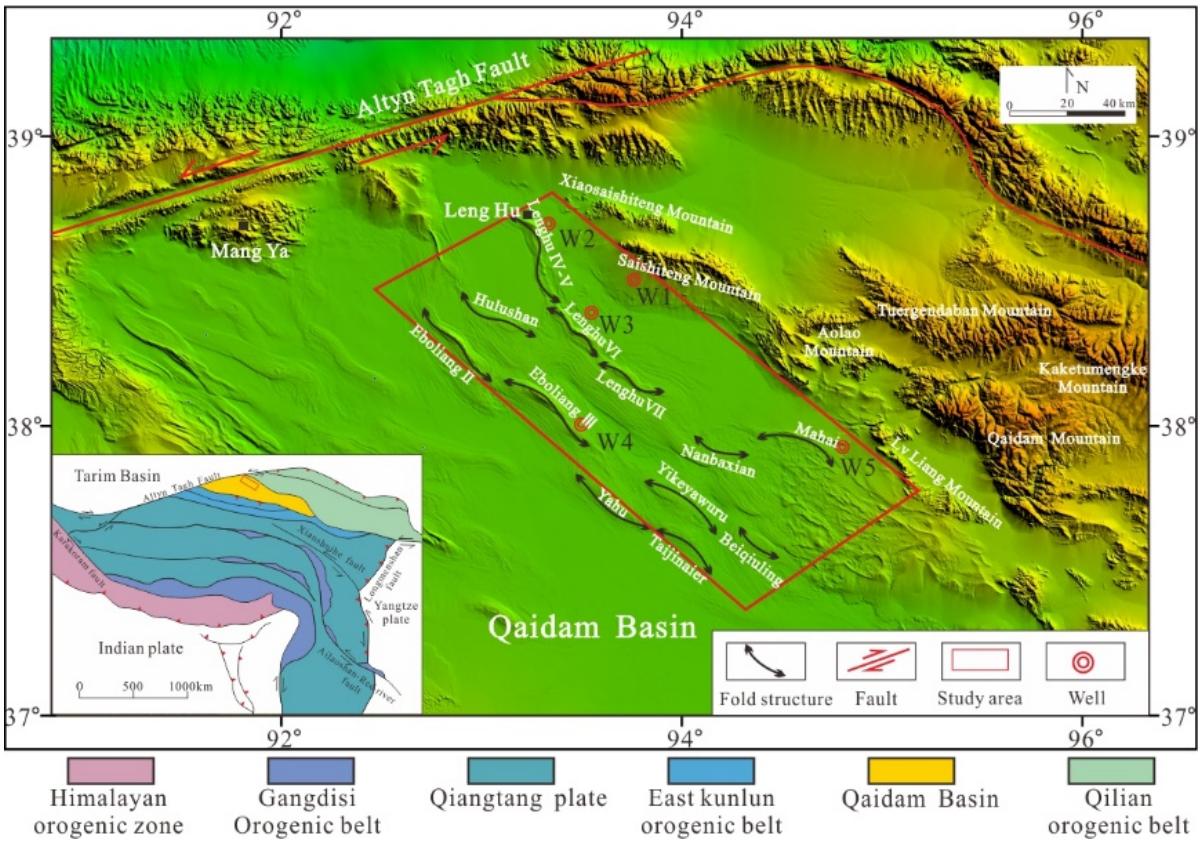

Figure 1. Structural location of the northern margin of Qaidam Basin.

The Cenozoic strata are mainly exposed in the northern area of Qaidam Basin, where the Mesozoic strata are absent. The Cenozoic strata mainly include the following seven units (Figure 2) [17]: Lulehe Formation (Fm.) (>52–45 Ma); Xiaganchaigou Fm. (45–35.5 Ma); Shangganchaigou Fm. (35.5–22 Ma); Xiayoushashan Fm. (22–15 Ma); Shangyoushashan Fm. (15–8 Ma); the Shizigou Fm. (8–2.8 Ma); and the Qigequan Fm. (<2.8 Ma).

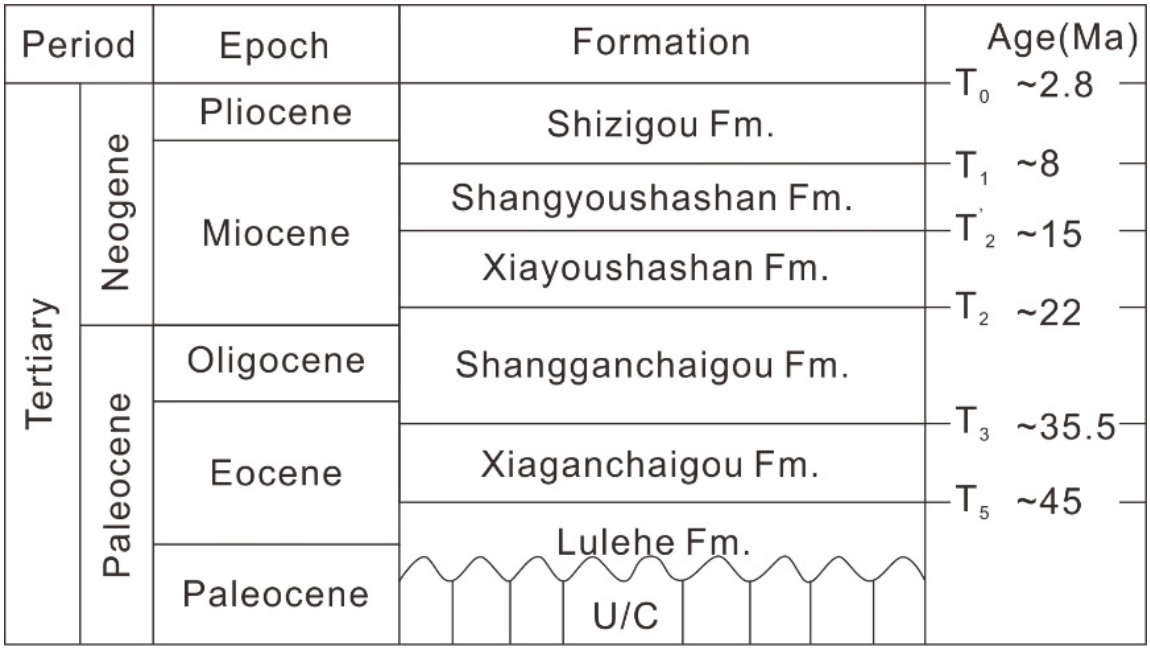

Figure 2. Paleogene–Neogene stratigraphy, seismic reflectors (T_0–T_5) of the northern Qaidam Basin Adapted with permission from Ref. [17]. Copyright 2013 Elsevier.

The northern margin of Qaidam Basin mainly includes Eboliang II, Eboliang III, Ikyauru, Hulushan, Lenghu IV to Lenghu VII, Beiqiuling, and Mahai–Nanbaxian thrust belts (Figure 1) [12]. From the Paleogene to Neogene, the Qaidam Basin experienced three stages: (1) during the Paleocene and early Eocene, the lake basin was formed; (2) during the late Eocene to Oligocene, the paleolake continuously expanded and reached its maximum extent; (3) during the Early Miocene to Pliocene, the paleolake then gradually shrank [12]. The sedimentary environments of the deep lake to semi-deep lake, shallow-shore lake, braided river, and braided river delta were developed in the northern margin of Qaidam Basin.

3. Samples and Methods

In this study, 150 core lutites samples were collected from five exploration wells in the northern margin of the Qaidam Basin (Figure 3) for observation, description, thin section identification, carbon and oxygen isotope and elemental geochemistry determination, etc. The analysis and testing of carbon and oxygen isotopes and trace elements were carried out in the Key Laboratory of Oil and Gas Resources Research, Northwest Institute of Eco-Environment and Resources, Chinese Academy of Sciences. The main elements were analyzed by fluorescence spectrometer 3080E3X in the Key Laboratory of Mineral Resources in Western Gansu Province.

Before carbon and oxygen isotope determination, the samples were titrated with dilute hydrochloric acid, most of which bubbled violently, indicating that the carbonate cement was mainly calcite. Then, the morphology and characteristics of carbonate cement were observed by polarizing microscope, and the sample of single carbonate cement was selected for carbon and oxygen isotope determination. The samples were crushed to 100 mesh, and tested by Delta V-Gasbench II Isotope Mass Spectrometer of Thermo Fisher, USA. The test results were obtained using international standard NBS-18 ($\delta^{13}C_{VPDB}$: −5.014, $\delta^{18}O_{VPDB}$: ±23.2) [18–21] and national standard GBW04405 ($\delta^{13}C_{VPDB}$: +0.57, $\delta^{18}O_{VPDB}$: −8.49), GBW04406 ($\delta^{13}C_{VPDB}$: −10.85, $\delta^{18}O_{VPDB}$: −12.4). After correction, the analysis accuracy was less than 0.1‰ with VPDB standard.

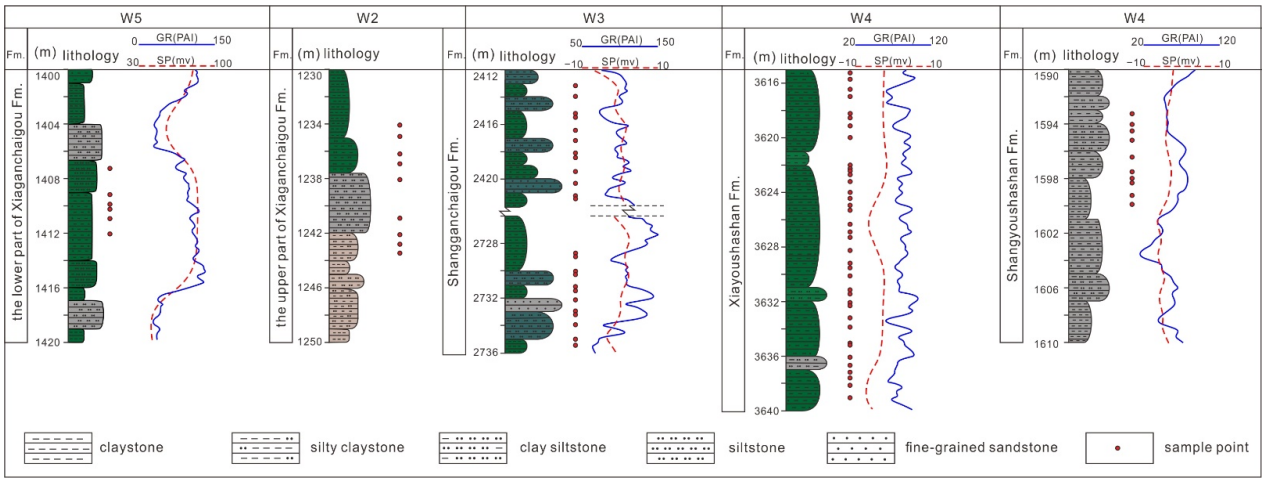

Figure 3. Cenozoic stratigraphic sequence, sample points and petrophysical characteristics of W2 well to W5 well in the northern margin of Qaidam Basin.

The mineral composition and structure of all of the samples in this study were observed under the microscope before the analysis of major and trace elements to ensure that the samples used for elemental geochemical analysis were not altered, mineralized, or subject to secondary weathering. All of the samples were ground with a non-polluting crushing machine and sifted through a 200-mesh sieve. After that, the samples were dried in the oven for about 3 h to remove moisture so that they could be accurately weighed. The fluorescence spectrometer 3080E3X produced by the Japanese Science Company was used for the determination of the main elements. HF + HNO_3 was used to seal and dissolve the samples for the analysis of trace elements, and the laser coupled plasma mass spectrometry (ICP-MS) was used for analysis and testing. The samples were analyzed and tested in the Key Laboratory of Oil and Gas Resources Research Center, Northwest Institute of Eco-Environment and Resources, Chinese Academy of Sciences.

4. Results

4.1. Stratigraphy

From log data, we drew five different columns with the main lithologies (Figure 3), five different lithologies were differentiated from claystone, silty claystone, clay silstone, siltstone, and fine-grained sandstone.

4.2. Carbon and Oxygen Isotopes

Carbon and oxygen isotopes in the different lutites' layers in the center of the northern margin of Qaidam Basin vary greatly, and the variation trend of carbon and oxygen isotopes is consistent. The Lulehe Fm. (five samples, Figure 4) shows $\delta^{13}C$ ranging from −7.8‰ to −2.4‰, with an average of −4.41‰, and $\delta^{18}O$ ranging from −13.4‰ to −10.7‰ with an average of −12.56‰. Carbon and oxygen isotopes of the lower part of the Xiaganchaigou Fm. (17 samples, Figure 4) and the upper part of Xiaganchagou Fm. (42 samples, Figure 4) show little variation (Figure 5), with $\delta^{13}C$ values ranging from −8.01‰ to −5.70‰ and from −8.71‰ to −3.78‰, with average values of −6.4‰ and −5.24‰, respectively, and $\delta^{18}O$ contents between +15.35‰~+11.16‰ and +16.62‰~+8.77‰, with average values of 13.19‰ and 13.30‰, respectively. The range of $\delta^{13}C$ in Shangganchaigou Fm. (31 samples, Figure 4) is from −6.81‰ to −3.80‰, with the average −5.34‰, the $\delta^{18}O$ value is from −12.73‰ to −6.98‰, with the average of −9.94‰. The variation ranges of carbon and oxygen isotopes in Xiayoushashan Fm. (39 samples, Figure 4) is similar to that in Shanggan-chaigou Fm., with $\delta^{13}C$ ranging from −7.37‰ to −3.24‰, with an average of −5.00‰, and $\delta^{18}O$ ranged from −10.57‰ to −0.93‰, with an average of −8.19‰. The Shangyoushashan Fm. (16 samples, Figure 4) shows $\delta^{13}C$ ranging from −7.37‰ to −3.57‰, with an average of −5.13‰, and $\delta^{18}O$ ranging from −9.78‰ to −6.34‰, with an average of −8.17‰.

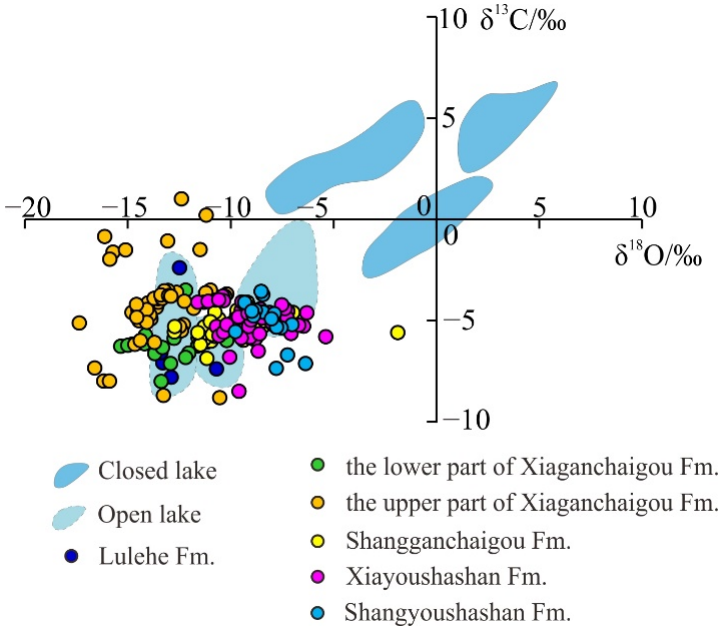

Figure 4. $\delta^{13}C$ and $\delta^{18}O$ values of the studied samples and water environment discrimination [22].

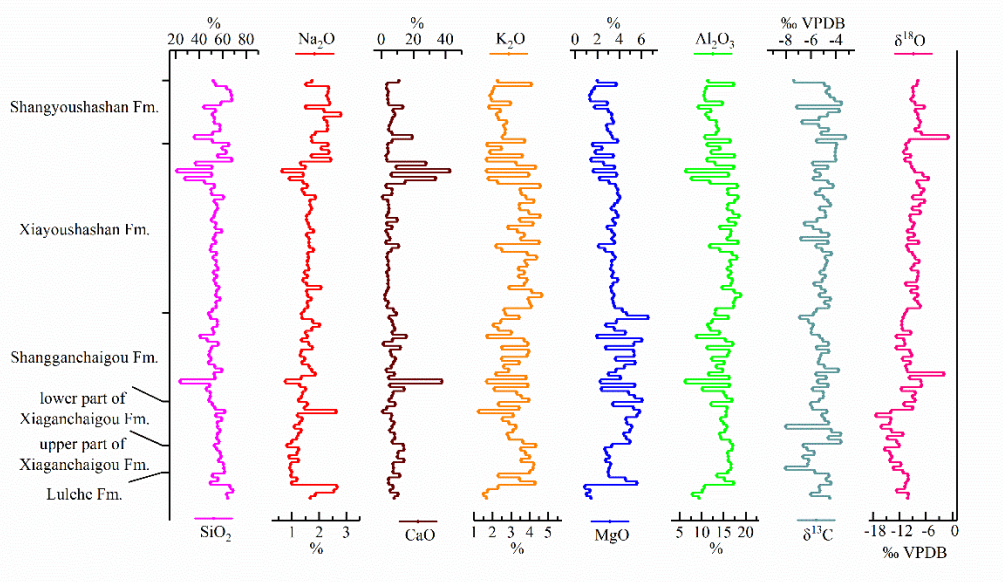

Figure 5. Variation trend of major elements and carbon and oxygen isotopes of the lutite samples in the study area.

4.3. Major and Trace Elements

Major and trace elements in different layers (Table 1) show that SiO_2 is the most abundant in all of the lutite samples, followed by Al_2O_3, CaO, Fe_2O_3, K_2O, Na_2O, and MgO, the former being less than 5%. As can be seen from the variation curve of major elements (Figure 5), the values of CaO, Al_2O_3, MgO, and K_2O have the same variation trend, while the contents of Na_2O and SiO_2 have opposite variation trends. Among them, the Lulehe Fm. samples had the highest SiO_2 contents, with an average of 59.89%, while the Shangganchaigou Fm. samples had the lowest SiO_2 contents, with an average of 50.73%. Na_2O and SiO_2 contents from Lulehe Fm. to Shangganchaigou Fm., and then Shangganchaigou Fm. to Xiayoushashan Fm., show first a decreasing trend, and then an increasing trend, while the variation trends of CaO, Al_2O_3, MgO, and K_2O contents are the opposite.

Table 1. Major elements of Paleogene-Neogene samples in the northern margin of Qaidam Basin.

Element Formation Samples		Lulehe *n* = 7	Lower Part of Xiaganchaigou *n* = 8	Upper Part of Xiaganchaigou *n* = 9	Shangganchaigou *n* = 27	Xiayoushashan *n* = 44	Shangyoushashan *n* = 17
range	SiO_2(%)	49.43–66.35	53.13–61.43	54.12–61.89	23.86–59.32	20.99–67.85	35.86–67.86
average		59.89	58.09	56.81	49.74	52.76	55.22
range	Al_2O_3 (%)	7.95–17.28	15.85–16.92	14.07–16.42	6.3–17.11	6.41–18.84	9.22–16.51
average		12.00	16.40	15.16	13.64	15.59	12.43
range	MgO (%)	0.86–5.59	2.69–3.35	4.40–5.88	1.96–6.61	1.42–4.06	1.31–3.87
average		2.55	3.01	4.99	4.31	3.21	2.69
range	CaO (%)	4.55–11.65	7.29–14.15	0.91–8.57	1.19–37.87	0.78–42.76	3.29–19.44
average		7.49	10.60	6.34	8.40	6.88	7.03
range	Na_2O (%)	0.96–2.55	0.82–1.26	0.99–2.64	0.75–2.03	0.91–2.44	1.49–2.81
average		1.70	1.03	1.37	1.49	1.62	2.11
range	K_2O (%)	1.5–3.46	3.51–4.33	1.25–3.63	1.68–3.97	1.68–4.66	1.8–4.09
average		2.47	3.94	2.83	2.96	3.44	2.53
range	Fe_2O_3 (%)	-	5.73–6.59	5.86–7.68	2.74–9.18	2.09–9.09	2.93–7.81
average		-	6.31	6.83	6.15	6.50	5.09
range	$\delta^{13}C_{VPDB}$	−7.8~−2.4	−8.01~−5.70	−8.71~−3.78	−6.81~−3.80	−6.81~−3.97	−7.37~−3.24
average		−4.41	−6.40	−5.24	−5.34	−5.00	−5.02
range	$\delta^{18}O_{VPDB}$	−13.4~−10.7	−15.35~−11.16	−16.62~−8.77	−12.73~−6.98	−11.1~−5.38	−9.78~−0.93
average		−12.56	−13.19	−13.30	−9.94	−8.63	−7.75

Trace elements are shown in Table 2. The contents of Sr, Ba, and Zn are relatively high compared with other trace elements, and the average contents are greater than 100 ppm. The variation trends of V, Cr, Co, and Ni contents are similar (Figure 6), with a clear positive correlation. The total amount of trace elements in Lulehe Fm. and Xiaganchaigou Fm. is relatively lower than the amounts in Shangganchagou Fm. and Xiayoushashan Fm. Before Paleogene, the variation range of Rb was relatively small, but in Neogene the content of Rb is higher.

Table 2. Trace elements of lutite samples in the northern margin of Qaidam Basin.

Formation Samples Element	Lulehe	Lower Part of Xiaganchaigou	Upper Part of Xiaganhcaigou	Shangganchaigou	Xiayoushashan	Shangyoushashan
	***n* = 7** **Range** **Average**	***n* = 14** **Range** **Average**	***n* = 24** **Range** **Average**	***n* = 27** **Range** **Average**	***n* = 44** **Range** **Average**	***n* = 17** **Range** **Average**
V (ppm)	39.36–140.47 69.21	32.35–70.20 46.77	14.36–97.24 39.88	30.9–131.8 91.95	42.6–121.6 95.85	45.9–100.1 72.91
Cr (ppm)	54.7–103.28 73.61	29.14–61.62 43.9	26.23–86.17 49.4	30.1–107.2 74.43	18.6–99.7 74.48	45.7–80.5 59.96
Co (ppm)	5.9–20.49 11.03	2.23–8.97 4.22	3.16–13.99 7.05	2.7–30.2 17.77	7.5–34.8 20.39	5.4–22.3 12.14
Ni (ppm)	10.14–61 27.41	3.44–11.22 7.33	4.99–29.03 13.54	2.3–150.5 46.64	12.0–85.8 44.33	5.7–79.9 29.48
Cu (ppm)	10.7–33.57 20.83	7.06–15.72 9.94	6.32–28.91 13.64	13.9–66.6 31.54	9–58.6 18.58	10.3–67.3 26.59
Zn (ppm)	25.81–118.48 55.85	8.88–49.91 19.08	19.58–103.51 46.61	42.5–150.9 99.8	44.8–133.2 97.69	44.8–102.8 70.99
Rb (ppm)	53.23–98.9 77.43	55.84–113.82 73.17	57.28–144.99 82.45	47.8–148.8 106.15	142.7–660.2 235.44	185.2–462.3 256.34
Sr (ppm)	132.27–227.13 172.28	120.66–206.03 137.25	85.53–152.88 115.75	162.2–876.2 279.71	44.5–167.3 126.94	55.7–150.2 96.88
Ba (ppm)	431.11–622.13 509.64	400.82–1835.48 736.71	271.9–1402.61 527.94	223.5–1856.4 862.25	323.7–1594.8 590.9	421.1–1297.7 683.54
Y (ppm)	9.21–26.46 17.85	4.37–16.24 10.14	6.56–26.27 13.5	15.3–26.4 22.85	16–29.7 25.04	15.1–25.7 21.75
Zr (ppm)	99.53–331.5 224.64	60.36–173.87 119.39	71.74–334.93 165.66	91.5–246.4 138.41	79–203.7 145.02	114.4–230.3 165.39
Nb (ppm)	3.91–14.05 9.68	2.77–8.48 5.13	2.84–13.43 6.47	11.4–19.7 15.72	6.9–22.8 15.68	10.8–31.2 16.85
La (ppm)	12.97–42.28 26.91	5.13–29.41 12.86	9.34–47.06 21.18	9.5–79.3 44.17	12.1–97.3 51.84	14–66.9 38.14
Pb (ppm)	9–29.34 15.22	7.77–18.76 12.59	6.6–31.33 11.76	6.5–37.6 20.59	7.3–41.2 18.4	1–67.2 21.01
MgO/CaO	0.1–1.2 0.44	0.02–0.66 0.24	0.09–5.52 0.65	0.16–4.47 0.82	0.04–5.21 0.83	0.13–1.05 0.46
Rb/Sr	0.33–0.67 0.46	0.31–1.03 0.56	0.03–1.29 0.70	0.07–0.83 0.49	0.87–5.65 1.70	1.23–5.43 2.82
V/Cr	0.67–1.36 0.89	0.76–1.40 1.09	0.43–1.49 0.75	0.99–1.52 1.23	0.81–2.29 1.32	0.90–1.62 1.22

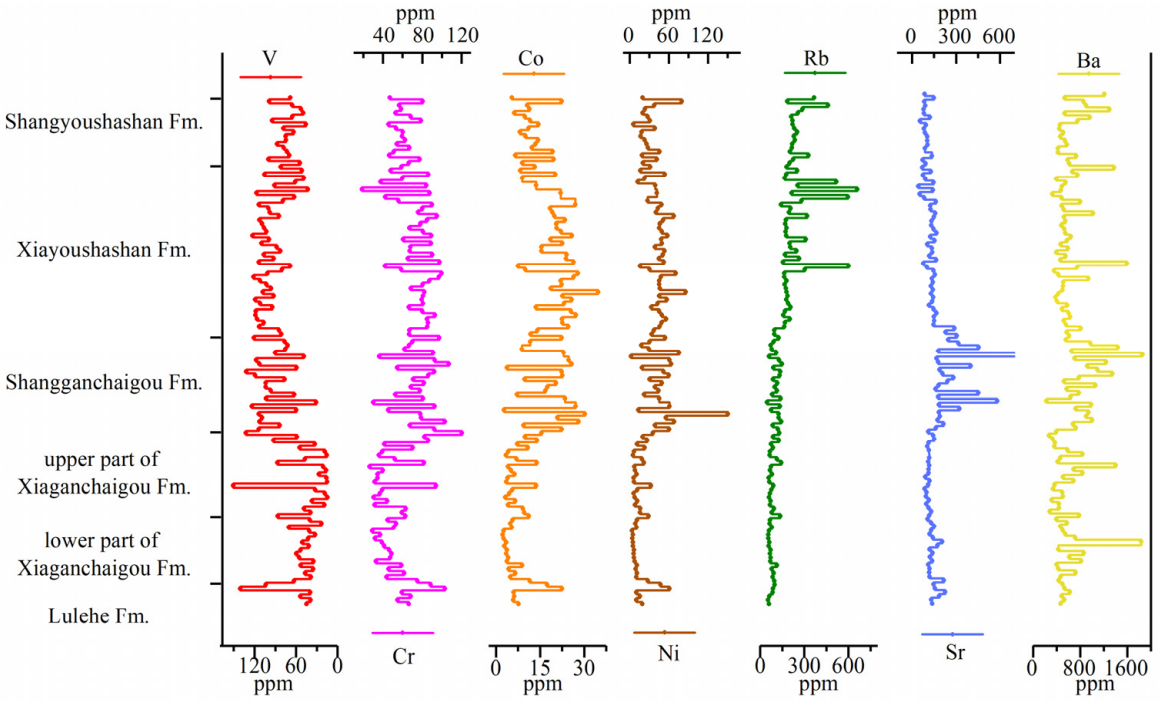

Figure 6. Variation trend of trace elements of lutite samples in the study area.

5. Discussion

5.1. Sedimentary Environment

The $\delta^{13}C$ of the study area decreased to the lowest in Lulehe Fm. and Xiaganchaigou Fm., and then increased significantly in the upper part of Xiaganchaigou Fm., after that, $\delta^{13}C$ remained relatively stable until the Xiayoushashan Fm. with little change (Figure 5). The $\delta^{18}O$ shows small variations in all of the samples. Studies show that the isotopic characteristics of primary carbonates may be used to distinguish between hydrologically open and closed lakes in the ancient lacustrine record [22]. The inflow-evaporation balance mainly dominates the composition of carbon and oxygen isotopes in closed lakes and highly correlated isotopic covariance is typical of carbonates from closed lakes [22]. Temperature effects are apparently of secondary importance in these closed lakes. In hydrologically open lakes, the carbon and oxygen isotopic compositions do not have a single relationship and the carbonates display small variations in $\delta^{18}O$ but relatively large changes in $\delta^{13}C$ [22]. Figure 4 shows that almost all of the samples fall in the third quadrant, indicating that the center of the northern margin of Qaidam Basin, from Lulehe Fm. to Shangyoushashan Fm., has always been in an open water environment. Sun et al. [23] indicated that most of the study areas were braided river or braided river delta sedimentary facies. Therefore, precipitation and evaporation jointly control the composition of carbon and oxygen isotopes

5.2. Paleoclimate Change

High $CaCO_3$ levels in lutites in a close or semi-close inland lake during the early stages of chemical deposition represent an arid climate, whereas low $CaCO_3$ levels represent a relatively humid climate. Ca^{2+} and Mg^{2+} commonly exchange from one to another but the large ionic radius of Ca^{2+} enhances its migration. Thus, an environment enriched in Ca^{2+} is likely drier than an environment enriched in Mg^{2+} [12]. Rb/Sr ratio has a good correlation with the strength of the inflow flow into the lake, and, therefore, with the dry–wet changes of the paleoclimate [24,25]. Rb has a large ionic radius. In continental basins, due to strong chemical weathering under wet conditions, it is easy to precipitate it in large quantities and for it to be absorbed by clays. However, these clays do not remain in situ, but are mainly denuded and transported into lake deposits. At the same time, the dissolved Sr elements entering the lake basin are generally deposited in arid conditions, so the Rb/Sr ratio is

high in a humid environment, that is, the high Rb/Sr ratio represents a humid climate environment, and a low ratio represents arid climate conditions. The good correlation between the Rb/Sr ratio and the MgO/CaO ratio of the studied samples (Figure 7) allows us to decipher the climate changes.

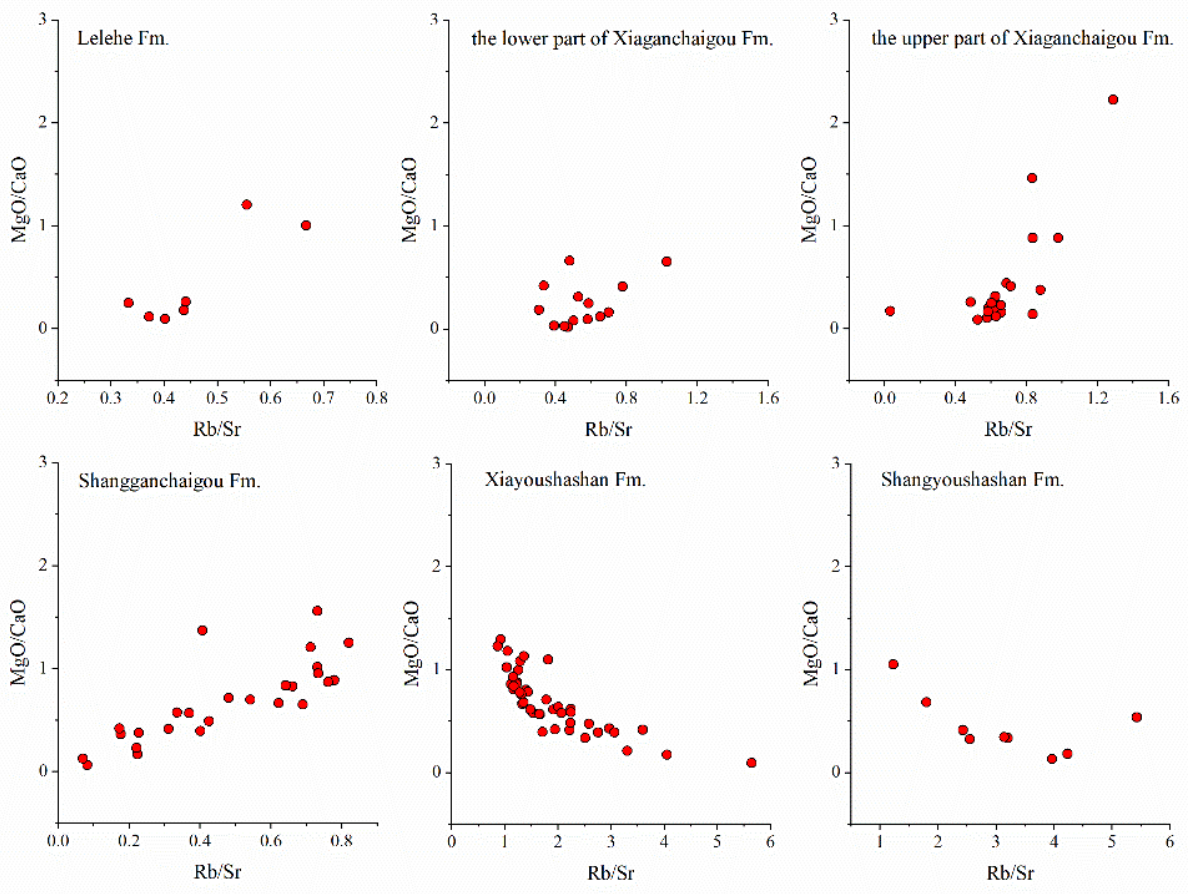

Figure 7. Correlation between Rb/Sr and MgO/CaO of the lutite samples in the study area.

The MgO/CaO ratio in the Lulehe Fm. in the northern margin of the Qaidam Basin ranges from 0.1 to 1.2, with an average of 0.44, and the Rb/Sr ratio ranges from 0.33 to 0.67, with an average of 0.46. The ratios of MgO/CaO and Rb/Sr in the lower part of Xiaganchaigou Fm. vary from 0.02 to 0.66 and from 0.31 to 1.03, with average values of 0.24 and 0.56, respectively. The decrease of MgO/CaO from Lulehe Fm. to the lower part of Xiaganchaigou Fm. indicates that the northern margin of the Qaidam Basin was in an arid climate during this period. The ratios of MgO/CaO and Rb/Sr in the upper part of Xiaganchaigou Fm. vary from 0.09 to 2.22 and from 0.49 to 1.29, with average values of 0.42 and 0.68, respectively. Compared with the lower part of the Xiaganchaigou Fm., MgO/CaO and Rb/Sr in the upper part of the Xiaganchaigou Fm. vary significantly, indicating that the climate was unstable, with alternate arid and humid climate but with an overall climate changing to a moist climate. The MgO/CaO ratio of Shangganchaigou Fm. ranges from 0.16 to 1.56, and the Rb/Sr ratio varies from 0.07 to 0.82, with an average of 0.67 and 0.47. The climate of Shangganchaigou Fm. alternately changed from wet to dry. As a whole, the sedimentary climate of Shangganchaigou Fm. was humid. The MgO/CaO ratio of the Shangyoushashan Fm. ranges from 0.09 to 5.21, with an average value of 0.89. The Rb/Sr ratio varies from 0.87 to 5.65, with an average content of 1.70. The climate of Shangyoushashan Fm. was unstable, with alternate dry and wet periods, although the whole period was in a relatively humid stage. The MgO/CaO and Rb/Sr ratios of Xiayoushashan Fm. vary from 0.13 to 1.05 and from 1.23 to 5.43, with average values of 0.46 and 2.28, respectively. In the Xiayoushashan Fm., MgO/CaO decreases gradually, but

the variation range is small, and Rb/Sr is relatively high on the whole, indicating that the climate was warm and humid.

In lacustrine sediments without seawater intrusion, Sr/Cu values between 1 and 10 indicate a warm and humid climate, while those higher than 10 indicate a dry and hot climate [26]. The results show that the Sr/Cu of most samples in Lulehe Fm. are between 1 and 10, which indicate that the climate was warm and humid. The Sr/Cu ratio of the lower part of Xiaganchaigou Fm. is more than 10, which is less than 10 in the early stage of the upper part of Xiaganchaigou Fm, and more than 10 in the late stage, indicating that the climate gradually became dry and hot from warm and humid. The Sr/Cu of Shangganchaigou Fm. Is ranged from 4.89–15.45 and most of them are lower than 10, except one sample is 36.97. In the early stage of Xiaganchaigou Fm., the Sr/Cu is more than 10. From the upper part of Xiaganchaigou Fm. to Youshashan Fm., the Sr/Cu frequently changes around 10, which indicates that the climate has suffered frequent changes from a dry and hot climate to warm and humid climate. From the late Xiayoushashan Fm. to the Shangyoushashan Fm., the Sr/Cu is less than 10, indicating that the climate was relatively stable, warm and humid (Figure 8).

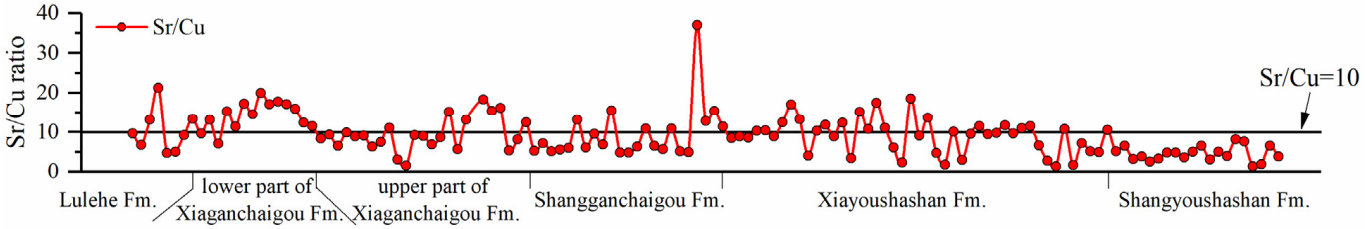

Figure 8. Sr/Cu climate discrimination diagram of lutite samples in the study area.

V became enriched in reduction conditions, while Cr became enriched in an oxidizing environment [27]. Therefore, the oxidation-reduction environment of the sediments can be inferred according to the V/Cr ratio. In the reductive sedimentary environment, the V/Cr ratio is >2, while in the oxidative environment, the V/Cr ratio is <2 [27]. In the Lulehe Fm., the V/Cr ratio ranges from 0.67 to 1.36 with an average of 0.89. The V/Cr ratio of the lower part of Xiaganchaigou Fm. ranges from 0.76 to 1.40 with an average of 1.09. In the upper part of Xiaganchaigou Fm., the V/Cr ranges from 0.43 to 1.49, with an average of 0.75, and in the Shangganchaigou Fm., the V/Cr ranges from 0.99 to 1.52, with an average of 1.23. Finally, in the Xiayoushashan Fm. and Shangyoushashan Fm., the V/Cr ranges from 0.81 to 1.64 and from 0.90 to 1.62, with an average ratio of 1.28 and 1.22 (Figure 9), respectively. All these values indicate that from Lulehe Fm. to Xiayoushashan Fm. sedimentation occurred in an oxidizing environment.

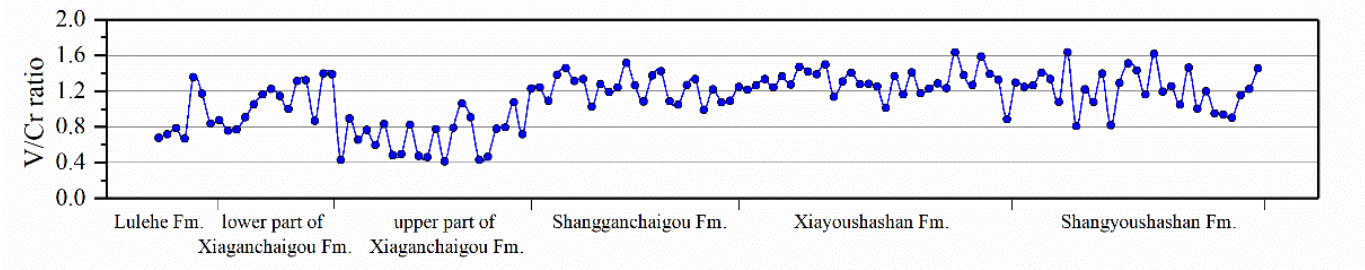

Figure 9. V/Cr oxidizing-reductive environment discrimination diagram of lutite samples in the study area.

The bulk chemical changes that take place during weathering were also used to quantify the weathering history of sedimentary rocks, and to understand past climatic

conditions [28]. The Chemical Index of Alteration (CIA) was established as a general guide to the degree of weathering:

$$CIA = Al_2O_3/(Al_2O_3 + CaO^* + Na_2O + K_2O) \times 100$$

where CaO* represents Ca in silicate-bearing minerals only [28]. According to Nesbitt and Young [29], CIA between 50 and 65 indicates a low degree of chemical weathering under cold and dry climatic conditions, CIA between 65 and 85 indicates moderate chemical weathering under warm and humid conditions, and CIA between 85 and 100 indicates intense chemical weathering under hot and humid extreme conditions. In the Lulehe Fm., the CIA values range from 58 to 76 (Figure 10), with an average value of 66, which represented a low to moderate degree of chemical weathering. The CIA of the lower part of Xiaganchaigou Fm. and the upper part of Xiaganchaigou Fm. is between 72 and74 and from 70 to 75, with average values of 73 and 73, respectively (Figure 10). These values indicate that Xiaganchaigou Fm. experienced moderate chemical weathering. The CIA of Shangganchaigou Fm. ranges from 65 to 72, with an average value of 69 (Figure 10). The CIA of Xiayoushashan Fm. and Shangyoushashan Fm. range from 68 to 72 and from 64 to 71, with average values of 70 and 66 (Figure 10), indicating moderate chemical weathering under warm and humid conditions.

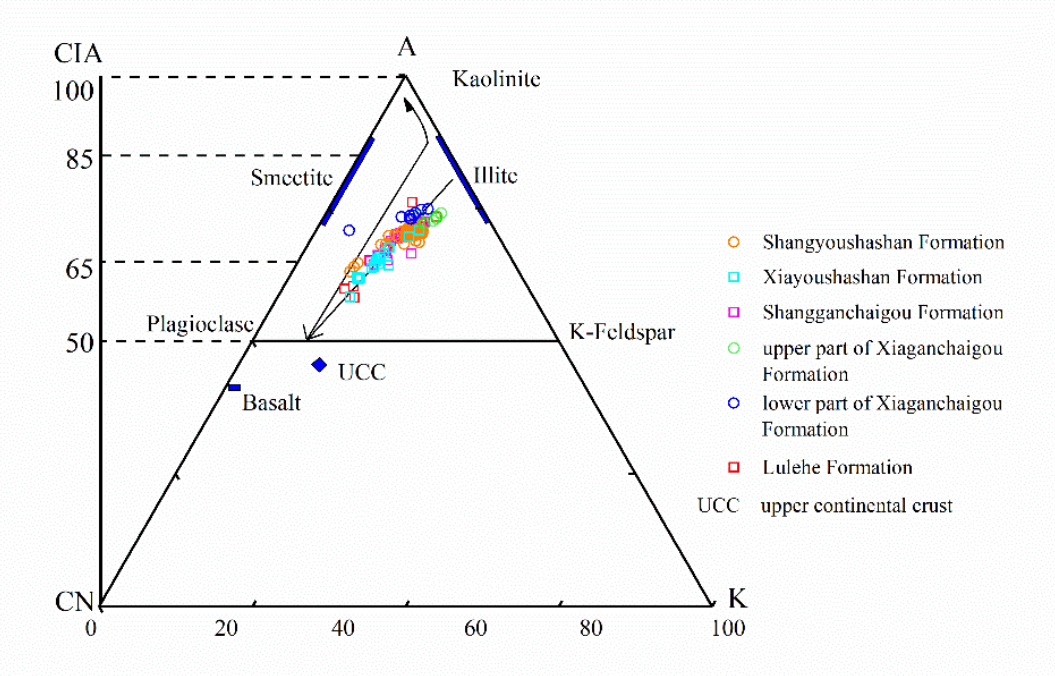

Figure 10. A–CN–K ternary diagram for lutites in the study area, A: Al_2O_3, CN: $CaO + Na_2O$, K: K_2O.

Climate is considered to be the critical factor affecting chemical maturity. Chemical maturity can be represented in terms of the chemical maturity index (CMI), which is expressed as a bivariant plot of SiO_2 against total $Al_2O_3 + K_2O + Na_2O$ [30]. In Figure 11, the sample points of Lulehe Fm. are located in semi-humid and semi-arid areas. The sample points of the lower and upper part of Xiaganchaigou Fm. are all in the arid area. Finally, the sample points of Shangganchaigou Fm., Xiayoushashan Fm. and Shangyoushashan Fm. are located in semi-arid and arid areas.

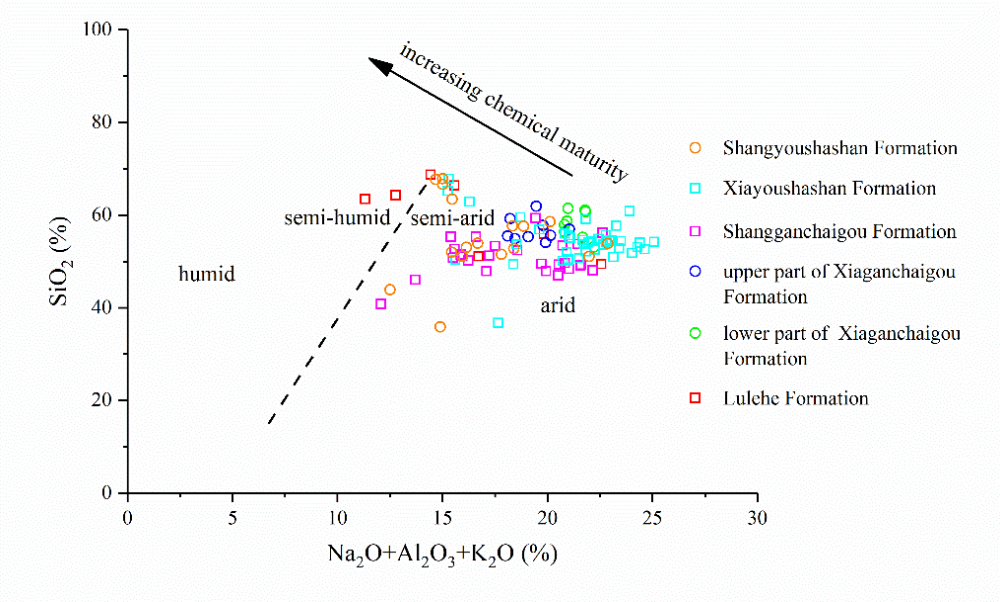

Figure 11. Chemical maturity of lutites' samples in the study area.

5.3. Response of Sand Body to Depositional Environment

Based on the above analysis, it can be concluded that in Paleogene the sedimentary characteristics of the Qaidam Basin gradually changed from warm and wet to cold and dry from Lulehe Fm. to the upper part of Xiaganchaigou Fm. The sedimentary environment of Neogene was characterized by the frequent alternation of arid and humid climate, and this is represented in the sedimentary record as the alternation of coarse sandstones and lutites in the northern margin of Qaidam Basin (Figure 12). During the arid and hot climate, the water supply into the lake decreased and evaporation increased, the accommodating space decreased, and the water level of the lake decreased. Under these regressive periods, the sandstone bodies usually show a reverse grain order (Figure 12b). During the warm and humid period, the water supplies increased, the accommodating space became larger, and the water level of the lake increased. During these periods of water inflow, the sandstone bodies present normal grading cycles (Figure 12a,c).

Figure 12. Outcrop views of (**a**) Lulehe Fm. showing normal grading sequences, from coarser to finer; (**b**) Xiaganchaigou Fm. showing reverse grading sequences, from finer to coarser; and (**c**) Shangganchaigou Fm. showing normal grading sequences in the northern margin of Qaidam Basin.

5.4. Sedimentary Environment Evolution Model

Based on the elemental geochemistry and isotope data of clastic rocks in the northern margin of Qaidam Basin, climate, chemical maturity, and chemical weathering were analyzed, and the evolution model of Cenozoic climate and sedimentary environment was established and divided into four evolution stages.

During the Paleocene–early Eocene (>52–45 Ma) (Lulehe Fm.), the Qaidam Basin was a large lake basin with no uplift in the surrounding mountains [15]. The basin may have been much larger than the present basin, but it was already the prototype of the present basin. The lake basin was an open lake. The sedimentary center of the lake basin was in the southwest of Qaidam Basin. Coarse clastic deposits such as conglomerates, pebbly sandstones, unsorted grain sandstones, and medium coarse grain sand-stones of alluvial fan braided river facies mainly developed in the northern margin of Qaidam Basin [5]. The grain size of the late Lulehe Fm. was finer, mainly composed of badly sorted fine to medium-grained sandstones, mixed with sandy lutites and lutites (Figure 12a). The changes in grain size indicate that the ancient landform during the sedimentation of Lulehe Fm. was characterized by a large topographic slope change, low water level, and small sedimentary lake area (Figure 13a). Rb/Sr and MgO/CaO results show that in the early Paleogene, the sedimentary environment was relatively warm and humid, with moderate chemical weathering. Previous studies [31] of sporopollen assemblage indicated that the vegetation type was common green broad-leaved forest, accompanied by thermophilic herbaceous plants, and a small number of small shrubs. In the late period of Lulehe Fm., the climate gradually became dry and cold (Figure 11), the proportion of wet-loving vegetation rapidly decreased, and the proportion of coniferous forest rapidly increased [31], which corresponded to the climate cooling event recorded by the global deep-sea oxygen isotope [32]. Meanwhile, the variation of $\delta^{18}O$ of Lulehe Fm. samples also shows a similar trend to the global deep-sea oxygen isotope, indicating that the climate in the Qaidam Basin was mainly affected by global climate change at this time.

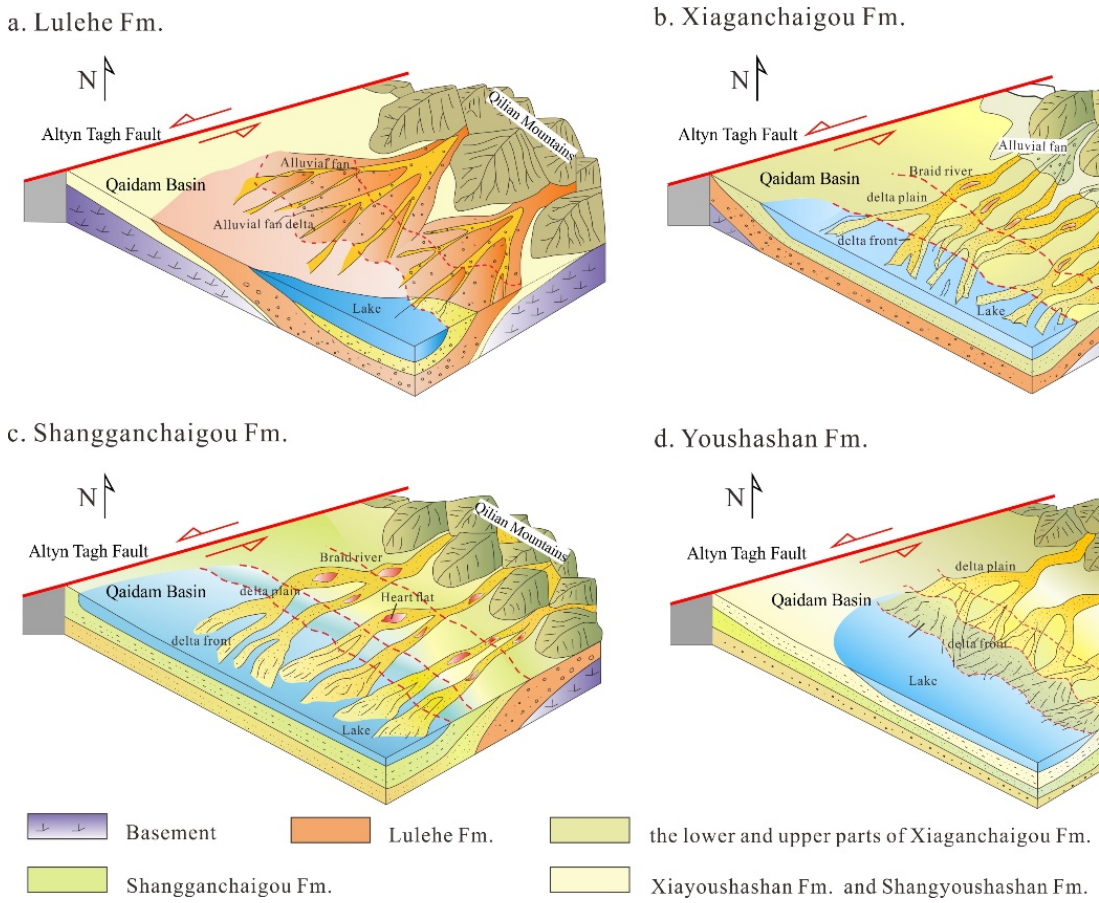

Figure 13. Cenozoic sedimentary environment evolution of the study area.

In the middle and late Eocene (45–35.5 Ma, Xiaganchaigou Fm.), due to the collision of the plates between the Indian plate and Europe plate, the first uplift of the Tibetan Plateau

took place [33]. The climate of the Qaidam Basin gradually became arid (Figure 11) and experienced the most intense chemical weathering (Figure 10). Braided rivers [23] were widely developed in the northern margin of Qaidam Basin (Figure 13b), which deposited a very thick layer of sediments consisting of conglomerates, pebbly conglomerates, coarse sandstones, fine-grained sandstones, siltstones, and lutites (Figure 12b). At this time, the elevation of the Qaidam Basin was 1000 m, mainly influenced by the subtropical high under the control of the planetary circulation system [31]. With the decrease in humidity, the vegetation type grew evergreen broad-leaved forest, and the drought-tolerant vegetation increased [31]. The temperature and humidity decreased, directly related to the overall collision with the Qinghai–Tibet Plateau [34,35].

During the late Eocene to the early Miocene (35.5–22 Ma, Shangganchaigou Fm.), the climate of the Qaidam Basin gradually changed from arid to semi-arid and semi-humid and experienced an alternation between arid, semi-arid, and semi-humid periods. The water level in the lake significantly increased. Braided river delta facies [36] widely developed in the northern margin of Qaidam Basin during this period (Figure 13c), originating a thick sequence of interbedded fine-grained sandstones and lutites. Sr/Cu and V/Cr showed that the climate alternated between dry and wet during this period (Figures 8 and 9). The palynological assemblage also shows that the climate had experienced many alternate processes of dry and wet cooling and warmth. In the early Oligocene, the vegetation changed from warm and humid evergreen broad-leaved and deciduous vegetation to drought-tolerant and cold-tolerant vegetation, and the climate gradually became arid [31]. In the middle Oligocene, the species and quantity of pollen of evergreen broad-leaved trees and evergreen deciduous plants increased and the proportion of xerophytic molecules decreased. In the late Oligocene, the content of evergreen broad-leaved trees decreased again, while the content of evergreen deciduous plants increased slightly, indicating that the temperature and humidity at that time decreased slightly again [31]. The climate was warm and humid with many periods of dry and wet fluctuations. Previous studies of clay minerals also indicate that there were wet-to-dry fluctuations during this period [37]. The climatic alternation during this period was mainly influenced by the uplift of the Tibetan Plateau and the remote effect of the collision of the Eurasian plate [38]. In addition, the rapid uplift and denudation of the Altun mountains at the south, revealed by cryogenic thermochronology studies, could have also been a factor affecting climate change [39].

From the late period of the early Miocene to the early period of the late Miocene (22–8 Ma, Xiayoushashan Fm. and Shangyoushashan Fm.), the geomorphic pattern of the Qaidam Basin was basically formed. The climate gradually changed from warm to dry. With the further decrease of river inflow and the continuous increase of evaporation, the lake water gradually became salty, and the lake basin area decreased. Small supply of fine-grained sandstones, siltstones, and claystones, were deposited in a shore-shallow lake-braided river delta environment (Figure 13d) [36]. The climate of the Xiayoushashan Fm. was warm and humid, with frequent alternation from wet to dry periods, which is consistent with the curve changes of oxygen isotopes in the deep sea [32], and was generally wetter than the Shangganchaigou Fm. Other authors demonstrate that warm-loving deciduous broad-leaved trees were well developed, conifer trees reproduced prolifically, and aquatic plants dominated the waterfront area, which represented a typical temperate coniferous and deciduous broad-leaved mixed forest vegetation type [31].

A previous study [40] shows that, before 8.4 Ma, there was a period dominated by montmorillonite with low crystallinity of illite, indicating warm and humid climate conditions. This climate was inconsistent with global climate change. It suggested that the whole period of Youshashan Fm. was affected by global climate change, but, due to the uplift of the Tibetan Plateau, there were local climate differences in the Qaidam Basin.

Finally, during the deposition of the Shangyoushashan Fm., the climate tended to be arid, which also agrees with the increase of xerophytic and mesophytic herbaceous shrubs [31].

6. Conclusions

The Cenozoic sedimentary environment evolution, the sedimentary processes and characteristics were reconstructed by analyzing the carbon and oxygen isotopes, major and trace elements. Carbon and oxygen isotopes, Rb/Sr, MgO/CaO, Sr/Cu, V/Cr, CIA, and CMI in the northern margin of Qaidam Basin are very sensitive to paleoclimatic environment changes. Combining our data with the previous research on sporopollen, we established the evolution model of Cenozoic sedimentary environment.

The evolution of the Cenozoic sedimentary environment in the Qaidam Basin can be divided into four stages: 1. In the Paleocene-Eocene (Lulehe Fm.), the sedimentary environment was relatively warm and humid in the early stage, and gradually became dry and cold in the late stage. The climate was mainly affected by global climate changes; 2. In the middle to late of Eocene (the lower and upper parts of Xiaganchaigou Fm.), the climate was the driest and the lake water level was the lowest, probably due to the remote effect of plate collision; 3. In the late Eocene to the early Miocene (Shangganchaigou Fm.), the climate of the Qaidam Basin experienced several alternating changes from dry to wet and gradually became warm and humid, which is mainly attributed to tectonic effects; 4. In the late period of the early Miocene to the early period of the late Miocene (Xiayoushashan Fm. and Shangyoushashan Fm.), the Xiayoushashan Fm. experienced frequent climate changes, with alternate dry and wet climates, and was generally wetter than the Shangganchaigou Fm. During the Shangyoushashan Fm., the climate became generally arid, mainly due to the global climate change, but at the same time, due to the uplift of the Qinghai–Tibet Plateau, there were regional climate differences in the Qaidam Basin.

Author Contributions: Conceptualization, Y.W. and G.S.; methodology, S.Z. and H.G.; formal analysis, Y.W. and G.S.; investigation, S.Z., G.S. and S.B.; resources, G.S. and S.Z.; writing—original draft preparation, Y.W.; writing—review and editing, Y.W., D.C., V.B., I.C. and A.T.; supervision, S.Z.; project administration, S.Z. and A.T.; funding acquisition, Y.W., S.Z. and A.T. All authors have read and agreed to the published version of the manuscript.

Funding: This research was funded by the National Natural Science Foundation of China, grant No. 41872145 and the China scholarship council, grant No. 202104910423. This research also was carried out within the framework of the DGICYT Spanish project PGC2018-093903-B-C22 (Ministerio de Ciencia, Innovación y Universidades/Agencia Estatal de Investigación/10.13039/501100011033/Fondo Europeo de Desarrollo Regional, Unión Europea) and the Grup Consolidat de Recerca "Geologia Sedimentària" (2017-SGR-824). David Cruset acknowledges the Spanish Ministry of Science and Innovation for the "Juan de la Cierva Formación" fellowship FJC2020-043488-I AEI/10.13039/501100011033.

Institutional Review Board Statement: Not applicable.

Informed Consent Statement: Not applicable.

Data Availability Statement: Not applicable.

Acknowledgments: We would like to thank Yunjiang and Yongheng Yang for their helping in the field.

Conflicts of Interest: The authors declare no conflict of interest.

References

1. Song, B.; Xu, Y.; Liang, Y.; Jiang, S.; Luo, M.; Ji, J.; Fang, H.; Yi, W.; Xu, Z.; Jiang, G. Evolution of Cenozoic Sedimentary Basins in Western China. *Earth Sci. Front.* **2014**, *8*, 1035–1051.
2. Wang, C.; Zhao, X.; Liu, Z.; Lippert, P.; Graham, S.; Coe, R.; Haisheng, Y.; Zhu, L.; Liu, S.; Li, Y. Constraints on early uplift history of the Tibetan Plateau. *Proc. Natl. Acad. Sci. USA* **2008**, *105*, 4987–4992. [CrossRef] [PubMed]
3. Garzione, C. Surface uplift of Tibet and Cenozoic global cooling. *Geology* **2008**, *36*, 1003. [CrossRef]
4. Molnar, P. The growth of the Tibetan Plateau and Mio-Pliocene evolution of East Asian climate. *Palaeontol. Electron.* **2005**, *8*, 1–23.
5. Sun, G.; Wang, M.; Guo, J.; Wang, Y.; Yang, Y. Geochemical Significance of Clay Minerals and Elements in Paleogene Sandstones in the Center of the Northern Margin of the Qaidam Basin, China. *Minerals* **2020**, *10*, 505. [CrossRef]

6. Yang, Y.H.; Sun, G.Q.; Wang, Y.T.; Wu, J.; Jiang, Y.; Wang, M.; Li, J.S. Diagenesis and sedimentary environment of the lower Xiaganchaigou Formation deposited during the Eocene/Oligocene transition in the Lenghu tectonic belt, Qaidam Basin, China. *Environ. Earth Sci.* **2020**, *79*, 1–14. [CrossRef]
7. Gao, Y.; Wang, C.; Huang, Y.; Bin, H.U. Progress in the study of paleoclimate change in continental scientific drilling projects. *Earth Sci. Front.* **2017**, *24*, 229–241.
8. Melles, M.; Brigham-Grette, J.; Minyuk, P.S.; Nowaczyk, N.R.; Wennrich, V.; DeConto, R.M.; Anderson, P.M.; Andreev, A.A.; Coletti, A.; Cook, T.L.; et al. 2.8 Million Years of Arctic Climate Change from Lake El'gygytgyn, NE Russia. *Science* **2012**, *337*, 315–320. [CrossRef]
9. Sun, Y.; Mu, Z. Isotopic Geochemical Studies on Global Change. *Acta Scicentiarum Nat. Univ. Pekinesis* **2001**, *4*, 577–586.
10. Armstrong-Altrin, J.S.; Lee, Y.I.; Verma, S.P.; Verma, S.P. Geochemistry of Sandstones from the Upper Miocene Kudankulam Formation, Southern India: Implications for Provenance, Weathering, and Tectonic Setting. *J. Sediment. Res.* **2004**, *74*, 285–297. [CrossRef]
11. Yang, L.; Zhang, W.; Fang, X.; Cai, M.; Lu, Y. Aridification recorded by lithofacies and grain size in a continuous Pliocene-Quaternary lacustrine sediment record in the western Qaidam Basin, NE Tibetan Plateau. *Palaeogeogr. Palaeoclimatol. Palaeoecol.* **2020**, *556*, 109903. [CrossRef]
12. Sun, G.; Wang, Y.; Guo, J.; Wang, M.; Jiang, Y.; Pan, S. Clay Minerals and Element Geochemistry of Clastic Reservoirs in the Xiaganchaigou Formation of the Lenghuqi Area, Northern Qaidam Basin, China. *Minerals* **2019**, *9*, 678. [CrossRef]
13. Hao, Q.; Yang, S.; Song, Z.; Ran, X.; Yu, C.; Chen, C.; Van Zwieten, L.; Quine, T.A.; Liu, H.; Wang, Z.; et al. Holocene carbon accumulation in lakes of the current east Asian monsoonal margin: Implications under a changing climate. *Sci. Total Environ.* **2020**, *737*, 139723. [CrossRef] [PubMed]
14. Jia, Y.; Wu, H.; Zhu, S.; Li, Q.; Zhang, C.; Yu, Y.; Sun, A. Cenozoic aridification in Northwest China evidenced by paleovegetation evolution. *Palaeogeogr. Palaeoclimatol. Palaeoecol.* **2020**, *557*, 109907. [CrossRef]
15. Yin, A.; Dang, Y.-Q.; Wang, L.-C.; Jiang, W.-M.; Zhou, S.-P.; Chen, X.-H.; Gehrels, G.E.; McRivette, M.W. Cenozoic tectonic evolution of Qaidam Basin and its surrounding regions (Part 1): The southern Qilian Shan-Nan Shan thrust belt and northern Qaidam Basin. *Geol. Soc. Am. Bull.* **2008**, *120*, 813–846. [CrossRef]
16. Yin, A.; Dang, Y.Q.; Zhang, M.; Chen, X.H.; McRivette, M.W. Cenozoic tectonic evolution of the Qaidam Basin and its surrounding regions (Part 3): Structural geology, sedimentation, and regional tectonic reconstruction. *Geol. Soc. Am. Bull.* **2008**, *120*, 847–876. [CrossRef]
17. Jian, X.; Guan, P.; Zhang, D.W.; Zhang, W.; Feng, F.; Liu, R.J.; Lin, S.D. Provenance of Tertiary sandstone in the northern Qaidam basin, northeastern Tibetan Plateau: Integration of framework petrography, heavy mineral analysis and mineral chemistry. *Sediment. Geol.* **2013**, *290*, 109–125. [CrossRef]
18. Irving, F.; James, O.N.; Gerald, C. Two New Carbonate Stable-Isotope Standards. *Geostand. Geoanal. Res.* **1982**, *6*, 11–12. [CrossRef]
19. Coplen, T.B.; Brand, W.A.; Gehre, M.; Gröning, M.; Meijer, H.A.J.; Toman, B.; Verkouteren, R.M. New Guidelines for $\delta_{13}C$ Measurements. *Anal. Chem.* **2006**, *78*, 2439–2441. [CrossRef]
20. Hut, G. *Consultants' Group Meeting on Stable Isotope Reference Samples for Geochemical and Hydrological Investigations*; International Atomic Energy Agency (IAEA): Vienna, Austria, 1987.
21. Stichler, W. Interlaboratory comparison of new materials for carbon and oxygen isotope ratio measurements. *Elements* **1995**, *825*, 67–74.
22. Talbot, M.R. A review of the Palaeohydrological interpretation of Carbon and Oxygen isotopic ratios in primary lacustrine organic matter. *Earth Planet. Sci. Lett.* **1990**, *110*, 23–37. [CrossRef]
23. Sun, G.; Xie, M.; Zhang, Y.; Zhao, M.; Kang, J.; Shi, J. Sedimentary characteristics and evolution of Paleogene Lower Xiaganchaigou Formation in northern Mahai area, northern margin of Qaidam Basin (in Chinese with English abstract). *Lithol. Reserv.* **2011**, *23*, 56–61.
24. Sun, G.; Yin, J.; Zhang, S.; Lu, X.; Zhang, S.; Shi, J. Diagenesis and sedimentary environment of Miocene series in Eboliang III area. *Environ. Earth Sci.* **2015**, *74*, 5169–5179. [CrossRef]
25. Zuo, X.; Li, C.; Zhang, J.; Ma, G.; Chen, P. Geochemical characteristics and depositional environment of the Shahejie Formation in the Binnan Oilfield, China. *J. Geophys. Eng.* **2020**, *17*, 539–551. [CrossRef]
26. Liu, S.; Lin, G.; Liu, Y.; Zhou, Y.; Gong, F.; Yan, Y. Geochemistry of middle oligocene-pliocene sandstones from the Nanpu Sag, Bohai Bay Basin (Eastern China): Implications for provenance, weathering, and tectonic setting. *Geochem. J.* **2007**, *41*, 359–378. [CrossRef]
27. Cao, J.; Wu, M.; Chen, Y.; Hu, K.; Bian, L.; Wang, L.; Zhang, Y. Trace and rare earth element geochemistry of Jurassic mudstones in the northern Qaidam Basin, northwest China. *Geochemistry* **2012**, *72*, 245–252. [CrossRef]
28. McLennan, S.M.; Hemming, S.; McDaniel, D.K.; Hanson, G.N.; Johnsson, M.J.; Basu, A. Geochemical approaches to sedimentation, provenance, and tectonics. In *Processes Controlling the Composition of Clastic Sediments*; Geological Society of America: Boulder, CO, USA, 1993; Volume 284.
29. Nesbitt, H.W.; Young, G. Early Proterozoic climates and plate motions inferred from major element chemistry of lutites. *Nature* **1982**, *299*, 715–717. [CrossRef]
30. Suttner, L.J.; Dutta, P.K. Alluvial sandstone composition and paleoclimate; I, Framework mineralogy. *J. Sediment. Res.* **1986**, *56*, 329–345.

31. Lu, J.; Zhang, K.; Bowen, S.; Yadong, X.; Jianyu, Z.; Wei, H.; Daolai, Z. Paleogene-Neogene Pollen and Climate Change in Dahonggou Region of Qaidam Basin. *Geosci. Front.* **2020**, *34*, 732–744.
32. Zachos, J.; Pagani, M.; Sloan, L.; Thomas, E.; Billups, K. Trends, Rhythms, and Aberrations in Global Climate 65 Ma to Present. *Science* **2001**, *292*, 686–693. [CrossRef]
33. Zeng, Q.; Wang, B.; Xiluo, L.; Mao, G.; Liu, H.; Liu, G. Suture Zones in Tibetan and Tethys Evolution. *Earth Sci.* **2020**, *8*, 2735–2763.
34. Zeng, L.; Haisheng, Y.I.; Xia, G.; Yuan, T. Sedimentary Sequences and Implications for Paleoenvironment of Cenozoic Lacustrine Stromatolites, Qaidam Basin. *Geosci. Front.* **2017**, *40*, 1251–1258.
35. Zhang, K.; Wang, G.; Hong, H.; Xu, Y.; Wang, A. The study of the Cenozoic uplift in the Tibetan Plateau: A review. *Geol. Bull. China* **2013**, *32*, 1–18.
36. Kong, H.; Zhao, J.; Hou, Z.; Si, D.; Zai, Z.; Ma, J.; Shen, Y. Provenance analysis and sedimentary environment evolution of the Neogene in Eboliang III structure of Qaidam Basin. *J. Palaeogeogr.* **2015**, *17*, 51–62.
37. Yin, K.; Hong, H.L.; Li, R.B. Clay mineralogy and its palaeoclimatic indicator of the Late Oligocene and Early Miocene in Xunhua basin. *Geol. Sci. Technol. Form.* **2010**, *29*, 41–48.
38. Yin, A.; Dang, Y.Q.; Chen, X.H.; Wang, L.Q.; Jiang, W.M.; Jiang, R.B.; Wang, X.F.; Zhou, S.P.; Liu, M.; Li-Xie, M.A. Cenozoic evolution and tectonic reconstruction of the Qaidam Basin: Evidence from seismic profiles. *J. Geomech.* **2007**, *13*, 193–211.
39. Liu, Y.J.; Neubauer, F.; Genser, J.; Ge, X.H.; Takasu, A.; Yuan, S.H.; Chang, L.H.; Li, W.M. Geochronology of the initiation and displacement of the Altyn Strike-Slip Fault, western China. *J. Asian Earth Sci.* **2007**, *29*, 243–252. [CrossRef]
40. Hanlie, H.; Chaowen, W.; Yaoming, X.; Kexin, Z.; Ke, Y. Paleoclimate Evolution of the Qinghai-Tibet Plateau since the Cenozoic. *Earth Sci. (J. China Univ. Geosci.)* **2010**, *35*, 728–736.